 doi:10.20944/preprints201705.0148.v1

Densities and Refractive Indices of Potassium Carbonate -Based Deep Eutectic Solvents with Dual Hydrogen Bond Donors at Several Temperatures (293.15 to 343.15 K)

Hosein Ghaedi, Muhammad Ayoub*, Suriati Sufian, Azmi Mohd Shariff and Bhajan Lal

Department of Chemical Engineering, Universiti Teknologi PETRONAS, 32610 - Bandar Seri Iskandar, Perak, MALAYSIA

* Correspondence: Muhammad.ayoub@utp.edu; Tel.: +60-53687623

Abstract: Deep eutectic solvents (DESs) are known as tunable solvents. It is possible to prepare ternary deep eutectic solvent (TDES) are used for desired purpose by selecting the suitable molar ratio and components of mixture. Therefore, four DESs and two TDESs were prepared in this work. DESs and TDESs were prepared with potassium carbonate (PC) as a hydrogen bond acceptor (HBA) and three hydrogen bond donors (HBDs) such as glycerol (GL), ethylene glycol (EG) and 2-amino-2methyl-1-3-propanediol (AMPD) known as a hindered amine (HA). Binary DESs were PC-GL with molar ratios 1:10 and 1:16 and PC-EG with the same molar ratios. TDES were prepared by adding AMPD in binary DESs such as PC-GL-AMPD 1:16:1 and PC-EG-AMPD 1:10:1. The experimental density and refractive index of all DESs and TDESs were measured at the temperature of 293.15 to 343.15 K with an interval of 5 K. The effect of temperature, molar ratio and alkyl chain length on the properties was investigated. The molar volumes and isobaric thermal expansion were calculated using experimental density data. The experimental refractive index data was used to derive the specific refraction, molar refraction, free molar volume, electronic polarization, polarizability constant and internal pressure at several temperatures.

Keywords: DES; TDES; salt; HBD; density; refractive index.

1. Introduction

Deep eutectic solvents (DESs) are derived from two or more salts as the hydrogen bond acceptors (HBAs) and hydrogen bond donors (HBDs). Salts components are such as allyltriphenyl phosphonium bromide (ATPPB), allyltriphenyl phosphonium chloride (ATPPC), methyltriphenyl phosphonium bromide (MTPPB), methyltriphenyl phosphonium chloride (MTPPC), benzyltriphenyl phosphonium bromide (BTPPB), benzyltriphenyl phosphonium chloride (BMTPPC), choline chloride (ChCl) and potassium carbonate (PC). HBDs components are for example amides, amines, alcohols, and carboxylic acids. In 2003, Abbot et al. [1] introduced DESs by synthesis of urea and a range of quaternary ammonium salts.

Density of a solvent plays a very important role in studying its applicability in various field of studies. It is well known that density is a function of temperature. The increase in temperature results in more molecular activity and mobility. By increasing mobility, the molar volume of solution increases, consequently the density of solution decreases. For many application, it is very important to know the temperature effect on density [2].

 doi:10.20944/preprints201705.0148.v1

Refractive index is another important physical property, which specifies the dielectric response to an electrical field induced by electromagnetic waves (light) and is thus an optical property of materials [2; 3]. Refractive index values provide a satisfactory analytical method to determine the composition of solvents. These values are also used to evaluate molar refractions which describe the molecular interactions between the solutes present in a mixture. It is used for different purposes, for instance, in order to confirm the purity of materials, estimate the concentration of solutes in solutions and identify a particular substance [2].

Leron et al. [4] measured the density of choline chloride (ChCl)/ ethylene glycol (EG) or glycerol (GL) at several temperatures. They stated that the density and refractive index of DESs decrease as the temperature increase. Leron and Li [5] measured the density of ChCl/ urea over the temperature range (298.15 to 323.15) K and pressure up to 50 MPa. Their results disclosed that the densities decrease with an increase in temperature (at constant pressure) due to thermal expansion and increase with an increase in pressure (at constant temperature) because of volume compression.

The temperature dependence of both refractive index and density of DESs were reported by Hayyan et al. [2] for fructose based deep eutectic solvents, Mjalli et al. [6] for potassium carbonate based DESs, and Siongco et al. [7] in the cases of N,N-diethylethanol ammonium chloride–glycerol (DEACG), N,N-diethylethanol ammonium chloride–ethylene glycol (DEACEG) and Kareem et al. [3] for phosphonium based DESs. In addition, the effect of temperature on density was investigated by AlOmar et al. [8] for Glycerol-based deep eutectic solvents, Yadav and Pandey [9] for reline, Baoyou Liu and Yaru Liu [10] for acetamide-LiCl.

Florindo et al. [11] studied the effect of carboxylic group and length of alkyl chain on HBDs on density of DESs. Their results showed that the increase in the hydrocarbon chain on HBDs leads to a decrease in the density of the DES. Moreover, it was found that density of DESs increases as the number of carboxylic group in DESs increases. Hayyan et al. [2]. measured the density and refractive index of fructose-based DES of choline chloride at various temperatures (25–85 °C) and found that by increasing the salt molar ratio in mixtures, the density of the DESs decreases. However, this trend was not observed in the case refractive index values. Therefore, it can be said that temperature, the nature of salt and HBD, the amount of salt/HBD and alkyl chain length have a great effect on the density and refractive index of pure DESs.

On the other hand, in order to improve the features of DESs for desired application, researchers are trying to synthesize the ternary deep eutectic solvents (TDES), because DESs are known as tunable solvents [12]. Maugeri and de Marı´a [13] reported the synthesis of TDES including ChCl, bio-based HBDs and glycerol (GL) as second HBD and measured their viscosity. Dai et al. [14] prepared TDES with the name of the natural deep eutectic solvents (NADES) by mixing the several abundant constituents (primary metabolites) for example sugars, sugar alcohols, amino acids, organic acids, and choline derivatives. Wang et al. [15] formed TDES with the components of ChCl, urea and nickel chloride hexahydrate ($NiCl_2.6H_2O$) and measured the physicochemical properties. Liu et al. [16] synthesized several TDESs by mixing imidazolium halides, zinc halides and amides and reported the physicochemical properties. Sze et al. [17] synthesized seven TDES for CO_2 capture by mixing the ChCl, GL and different superbases. Khezeli and Daneshfar [18] synthesized two types of ChCl- based TDEs having ChCl, phenol, ethylene glycol and anhydrous iron (III) chloride ($FeCl_3$) and called magnetic deep eutectic solvents (MDESs). Sarkar and Sampath [19] reported a TDES based on acetamide, urea and gallium nitrate for the electrode position of gallium nitride/gallium indium

 doi:10.20944/preprints201705.0148.v1

nitride. Hence, it is possible and interesting to synthesize task specific ternary deep eutectic solvents (TSTDES) for especial purposes particularly CO_2 capture, by suitable combinations of salts and HBDs.

In the present work, four binary DESs and two new TDESs were synthesized by mixing salt such as potassium carbonate (PC) with some HBDs for instance glycerol (GL), ethylene glycol (EG), and 2-amino-2methyl-1-3-propanediol (AMPD) as a hindered amine. The binary DESs were PC- GL and PC- EG with molar ratios of 1:10 and 1:16. The TDESs were PC-GL-AMPD with molar ratio of 1:16:1 and PC-EG-AMPD with molar ratio 1:10:1. The experimental density and refractive index of HBDs, DESs and TDESs were measured at several temperatures from 293.15 to 343.15 K with an interval of 5 K. These experimental values were used to calculate the molar volume, isobaric thermal expansion, specific refraction, molar refraction, electronic polarization and internal pressure of DESs and TDESs.

2. Results and Discussion

Experimental Density, ρ, and refractive index, n_D values were correlated with temperature through a linear equation:

$$Y = a + b.(T) \tag{1}$$

where Y represents ρ and n_D; T is the absolute temperature; and a and b are empirical constants determined by fitting Equation (1) with the experimental values of ρ and n_D. The value of root mean square error (*RMSE*) for properties of DESs and TDESs studied here, is calculated by:

$$RMSE = \left[\frac{\sum \left(Y_{\text{exp}} - Y_{\text{pred}} \right)^2}{K - L} \right]^{0.5} \tag{2}$$

where Y_{exp} and Y_{pred} are experimental and predicted properties of all DESs and TDESs, respectively. K is the number of experimental data, and L is the number of parameters models including a and b.

2.1 Density property

Density is an important thermos-physical property owing to its effect on the design and operation of processes [6; 8; 20]. Hence, it is essential to identify the behavior of density with respect to temperature. In this work, the experimental density of the DESs, TDESs and their HBDs were measured in temperature range of 293.15 to 343.15 K at ambient pressure. The experimental density values of pure GL, pure EG, DESs and TDESs are tabulated in Table 1 and Figure 1 illustrates these values as a function of temperature. Table 2 represents a comparison between the density of HBDs such as GL and EG in this work and the literature data [21; 22]. Low values of average absolute deviation (%*AAD*) values indicate that there is consistency between experimental data and literature data, and the values are reproducible.

Preprints (www.preprints.org) | NOT PEER-REVIEWED | Posted: 19 May 2017 doi:10.20944/preprints201705.0148.v1

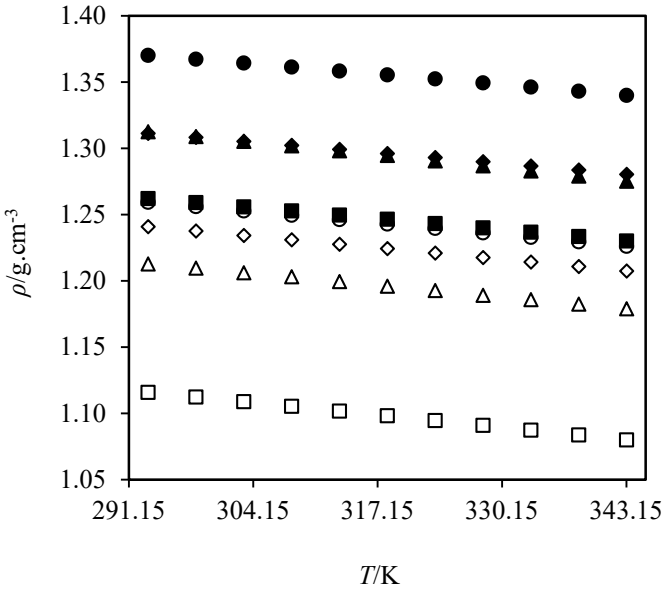

Figure 1. Experimental density, ρ, of the pure GL, pure EG, DESs and TDESs in this work, as a function of temperature: ■, pure GL; □, pure EG; ○, DES_1; Δ, DES_2; ◊, $TDES_1$; ●, DES_3; ▲, DES_4; ♦, $TDES_2$.

115

Table 1 . Experimental density, ρ, of pure GL, pure EG, DESs and TDESs. Measurements were conducted within temperature range from T = (293.15 to 343.15) K and p = 0.1 MPa.

	DESs and TDESs						**Pure component**	
	DES_1	**DES_2**	**$TDES_1$**	**DES_3**	**DES_4**	**$TDES_2$**	**EG**	**GL**
T/K	ρ/(g.cm^{-3})							
293.15	1.25933	1.21282	1.24090	1.37022	1.31252	1.31132	1.11578	1.26204
298.15	1.25606	1.20957	1.23763	1.36728	1.30890	1.30835	1.11230	1.25897
303.15	1.25277	1.20617	1.23431	1.36432	1.30528	1.30535	1.10878	1.25582
308.15	1.24948	1.20312	1.23098	1.36135	1.30196	1.30232	1.10524	1.25271
313.15	1.24618	1.19949	1.22766	1.35837	1.29813	1.29927	1.10169	1.24959
318.15	1.24287	1.19595	1.22432	1.35539	1.29461	1.29613	1.09812	1.24642
323.15	1.23954	1.19273	1.22096	1.35238	1.29058	1.29304	1.09453	1.24321
328.15	1.23619	1.18905	1.21759	1.34934	1.28679	1.28991	1.09092	1.23996
333.15	1.23282	1.18587	1.21420	1.34620	1.28290	1.28675	1.08728	1.23668
338.15	1.22947	1.18241	1.21083	1.34316	1.27911	1.28362	1.08362	1.23338
343.15	1.22610	1.17900	1.20744	1.34002	1.27522	1.28046	1.07994	1.23006

116

Preprints (www.preprints.org) | NOT PEER-REVIEWED | Posted: 19 May 2017 doi:10.20944/preprints201705.0148.v1

Table 2. Comparison of the experimental and the literature data of the density and refractive index of EG and GL.

	Ethylene glycol (EG)			Glycerol (GL)		
***T*/K**	**Exp.**	**Lit.**	**%*AAD*** [a]	**Exp.**	**Lit.**	**%*AAD***
	Density (ρ/g.cm^{-3})			Density (ρ/g.cm^{-3})		
293.15	1.11578	1.1140 [b]	0.11087	1.26204	1.26110 [c]	0.07307
298.15	1.11230	1.1120 [b]		1.25897	1.25802 [c]	
303.15	1.10878	1.1104 [b]		1.25582	1.25495 [c]	
	Refractive index			Refractive index		
298.15	1.430964	1.4292 [d]	0.1370	1.47182	1.4697 [f]	0.07343
303.15	1.429986	1.4287 [e]		1.47035	1.4710 [g]	
313.15	1.428224	1.4254 [e]		1.46747	1.4670 [g]	

[a] $\%AAD$ is the average absolute deviation and calculated: $\%AAD = \frac{100}{n} \times \sum_{i=1}^{i=n} \frac{\left|Y_{\exp} - Y_{\text{lit}}\right|}{Y_{\exp}}$

where Y_{exp} and Y_{lit} are experimental data and literature data, respectively; n represents the number of data point.

[b] [21].

[c] [22].

[d] [23].

[e] [24].

[f] [25].

[g] [26]

According to Table 1 and Figure 1, density values of HBDs (GL and EG) was less than those of corresponding DESs at all temperatures. As can be observed from the Figure 1, as the temperature increased the density of HBDs, DESs and TDESs decreased linearly. This could be attributed to the wider spaces between the mixture molecules and the increased molecular mobility at higher temperatures which increase the molar volume expansion and decrease the molecular interactions [7; 8; 27].

As shown in Figure 1, an increase in the mole fraction of GL and EG in the mixture, the density of DESs decreased. For example, the density of PC-GL 1:10 (DES4) is 1.36728 g.cm^{-3} while that of PC-GL 1:16 (DES5) is 1.30890 at 298.15 K. Similarly, the density of PC-EG 1:10 (DES1) and of PC-EG 1:16 (DES2) are 1.25606 and 1.20957 g.cm^{-3}. These observations were in a well agreement with the results obtain by Mjalli et al. [6] for potassium carbonate based DES together with GL and EG. Indeed, there are two possible reasons for this behavior. Firstly, the density of PC is about 2.285 g.cm^{-3} is less than those of GL (1.25897 g.cm^{-3}) and EG (1.11230 g.cm^{-3}). Therefore, by increasing the amount of GL and EG in the DES, the density of DESs decreased toward the density of the HBD which is the lower density in the mixture. Secondly, it is more likely that a decrease of hydrogen bond interactions in DESs leads to a decrease in density of DESs [27].

Preprints (www.preprints.org) | NOT PEER-REVIEWED | Posted: 19 May 2017 doi:10.20944/preprints201705.0148.v1

By adding AMPD to the binary mixture of PC-EG 1:10, the density of $TDES_1$ experienced a decreasing trend in the amount. For example, density of PC-EG 1:10 was 1.22610 $g.cm^{-3}$ at 343.15 K, while that of PC-EG-AMPD 1:10:1 was 1.20744 $g.cm^{-3}$ at the same temperature. This trend almost can be seen in the case of PC-GL-AMPD 1:16:1 ($TDES_2$) which had the higher density than PC-GL 1:16 at all temperatures except for 293.15 and 298.15 K.

At the same molar ratio of 1:10, PC-GL had the higher density value than PC-EG. This result is in a well agreement with the results reported by Mjalli et al. [6] who mentioned the density of PC-GL is higher than that of PC-EG with the same molar ratio of 1:6.

It is interesting to mention that as the molecular weight of DESs decreased the density of decreased provided that DESs have the same components but different molar ratio (see Table 11 for molecular weight and Table 1 and Figure 1 for density of DESs).

The experimental density values were fitted to linear relationship, as the following

$$\rho = a + b.(T) \quad (3)$$

where ρ is the density in $g.cm^{-3}$, T is the temperature in Kelvin, a and b are constant that depends on the type of DESs or TDESs. A method of least-squares was applied using the Levenberg-Marquardt algorithm to derive constant parameters (a and b) of Equation (3). The values of a and b for all DESs and TDESs together with $RMSE$ and R^2 values are shown in Table 3. We compared graphically the predicted density by Equation (3) with the experimental density data for all DESs and TDESs, as portrayed in Figure 2. From Figure 2, it is clear that the predicted density values for all DESs and TDESs were in a well agreement with experimental density data with R^2 values of >0.999, which indicated that the density–temperature relationships were linear.

Table 3 . The constant parameters of a, b used in Equation (3), $RMSE$ and R^2 values.

DES/TDES	a	$10^3 \times b$	$10^5 \times RMSE$	R^2
DES_1	1.454	-0.6646	5.926	0.99999
DES_2	1.412	-0.6791	14.4	0.9998
$TDES_1$	1.437	-0.6695	5.615	0.99999
DES_3	1.547	-0.6032	10.59	0.9999
DES_4	1.532	-0.7466	26.4	0.9996
$TDES_2$	1.493	-0.6182	10.61	0.9999

Preprints (www.preprints.org) | NOT PEER-REVIEWED | Posted: 19 May 2017 doi:10.20944/preprints201705.0148.v1

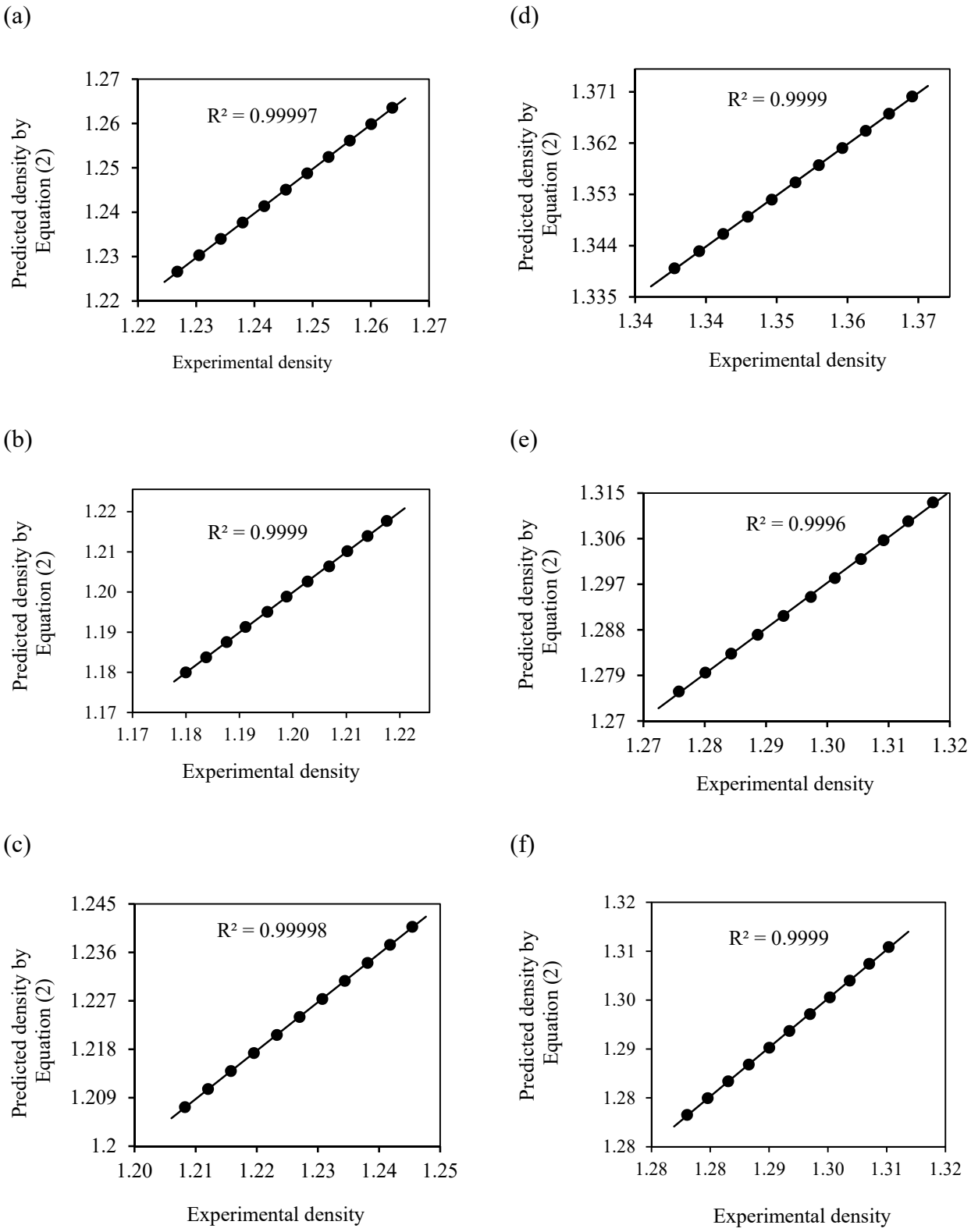

Figure 2. Comparison between the experimental and calculated values of density, ρ, for all DESs and TDESs: (a), DES_1; (b), DES_2; (c), $TDES_1$, (d), DES_3; (e), DES_4. ; (f), $TDES_2$.

Preprints (www.preprints.org) | NOT PEER-REVIEWED | Posted: 19 May 2017 doi:10.20944/preprints201705.0148.v1

The molar volume, V, of DESs and TDESs were calculated using the experimental density data for at different temperatures studied here, according to the following equation.

$$V = M/\rho \quad (4)$$

In the Equation (4), ρ and M are the density and molecular weight of DESs and TDESs. The molecular weight of DESs and TDESs are calculated according to the below equation [8; 28].

$$M = \frac{X_{\mathrm{HBA}} M_{\mathrm{HBA}} + X_{\mathrm{HBD}} M_{\mathrm{HBD}}}{X_{\mathrm{HBA}} + X_{\mathrm{HBD}}} \quad (5)$$

where M is the molecular weight of DES and TDES in g·mol^{-1}, X_{HBA} and M_{HBA} are the molar ratio and molecular weight of the salt as HBA in g.mol^{-1}, respectively; X_{HBD} and M_{HBD} are the molar ratio and molecular weight of the HBD in g.mol^{-1}, respectively. The temperature dependence of molar volume of DESs and TDESs are shown in Figure 3. Different from density property, the molar volume of DESs and TDESs increased with raising temperature.

The effect of molar ratio on the molar volume was investigated and it was found that by increasing the amount of HBDs in DES, the molar volume of DESs increased, however, this changing was not much in the case of PC-EG DESs, as shown in Figure 3 and Table 4.

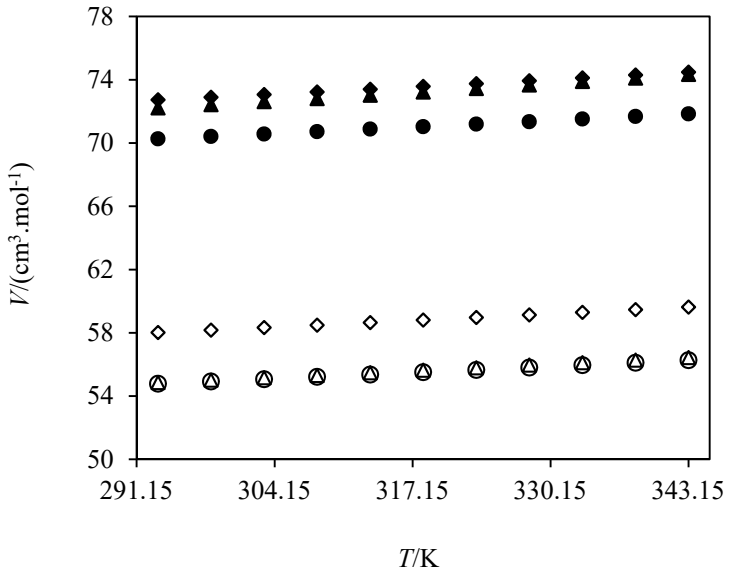

Figure 3. Molar volume, V, of DESs and TDESs as a function of temperature. The symbols are the same as symbols depicted in Figure 1.

Preprints (www.preprints.org) | NOT PEER-REVIEWED | Posted: 19 May 2017 doi:10.20944/preprints201705.0148.v1

Table 4 . Calculated molar volume, V, of DESs and TDESs within temperature range from T = (293.15 to 343.15) K and p = 0.1 MPa.[a]

	DESs and TDESs					
	DES$_1$	**DES$_2$**	**TDES$_1$**	**DES$_3$**	**DES$_4$**	**TDES$_2$**
T / K	V/(m^3.mol^{-1})					
293.15	54.7845	54.8711	58.0258	70.2681	72.2297	72.7338
298.15	54.9272	55.0186	58.1791	70.4192	72.4295	72.8989
303.15	55.0714	55.1737	58.3356	70.5720	72.6303	73.0664
308.15	55.2164	55.3135	58.4934	70.7259	72.8158	73.2364
313.15	55.3626	55.4809	58.6516	70.8811	73.0304	73.4083
318.15	55.5101	55.6452	58.8116	71.0369	73.2292	73.5862
323.15	55.6592	55.7954	58.9734	71.1950	73.4576	73.7620
328.15	55.8100	55.9681	59.1366	71.3554	73.6740	73.9410
333.15	55.9626	56.1181	59.3017	71.5219	73.8974	74.1226
338.15	56.1151	56.2823	59.4668	71.6837	74.1163	74.3033
343.15	56.2693	56.4451	59.6337	71.8517	74.3424	74.4867

2.2 Isobaric thermal expansion

The liquid contained in the equipment will expand if there is an increase in temperature. That is why it is essential to design a safety and relief system which will relieve (or emit) the thermally expanding liquid and hinder the pressure arise from this expansion. If the pressure increase is too much, the process equipment or apparatus will be damaged. Thus, thermal expansion coefficient, α_p / K^{-1}, data is important in process engineering [27; 29]. This property which provides the information of how much a component can expand with regard to temperature shows the fractional change in density when temperature increases at constant pressure. The temperature dependence of the isobaric thermal expansion coefficients, α_p / K^{-1}, were derived at different temperatures from the parameters obtained by the fitting of the experimental density data using Equation (3) and is calculated according to the following equation:

$$\alpha_p = \frac{1}{V}\left(\frac{\partial V}{\partial T}\right)_P = -\frac{1}{\rho}\left(\frac{\partial \rho}{\partial T}\right)_P = -\frac{b}{a+bT} \quad (6)$$

where ρ is the density of DESs and TDESs in g.cm^{-3}, T is the temperature in Kelvin, P is the ambient pressure, and a and b represent the parameters gained from the fitting of density data using Equation (3). Figure 4 depicts the temperature dependence of α_p for all DESs and TDESs. It can be clearly seen that temperature had not a great effect on α_p of DESs and TDESs. Moreover, there was a great effect on α_p of DESs due to changing in the amount of molar ratio in DESs. As can be seen from Figure 4, as the molar ratio of PC-EG and PC-GL DESs increased from 1:10 to 1:16, the amount of α_p of DESs increased especially in the case of PC-GL. It might be reasoned that a decrease of hydrogen bond interactions in DESs leads to a decrease in density, higher free volume of solvent (see Table 8 for free volume of DESs) and consequently raising the amount of isobaric thermal expansion coefficients [27].

Preprints (www.preprints.org) | NOT PEER-REVIEWED | Posted: 19 May 2017 doi:10.20944/preprints201705.0148.v1

215 On the other hand, by adding AMPD in PC-GL 1:16, the α_P values of PC-GL-AMPD ($TDES_2$) 1:16:1
216 decreased at all temperatures, while the α_P values of PC-EG-AMPD 1:10:1 ($TDES_1$) increased when
217 the AMPD was added in PC-EG 1:10.

218

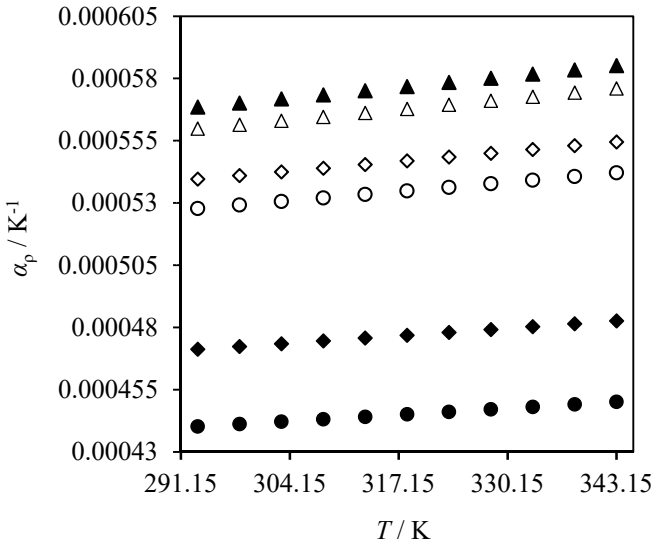

Figure. 4. Isobaric thermal expansion, α_Q, of DESs and TDESs at several temperatures of. The symbols are the as symbols depicted in Figure 1.

219

220 *2.3. Refractive index and derived properties*

221 Refractive index is a fundamental physical property of DESs and TDESs. The experimental
222 refractive index of DESs, TDESs and their HBDs were measured as a function of temperature and
223 repeated three times. The experimental refractive index values of pure GL, pure EG, DESs and TDESs
224 are listed in Table 5 and graphically shown in Figure 5. The refractive index of pure GL and pure EG
225 are compared with the literature data [23-26], as tabulated in Table 2. Low values of average absolute
226 deviation (%*AAD*) indicate the confirmation of the reproducibility of the experiments.
227 From the data represented in Table 5 and displayed in Figure 5, it is evident that pure GL has the
228 higher refractive index than pure EG in all temperature studied here.
229 There are several factors which have an effect on the refractive index of DESs and TDESs such as
230 type of salt/HBD, molar ratio, temperature and molecular weight. The results disclosed that the
231 values of n_D decreased with an increase in temperature, since temperature has an effect on the density
232 of the DESs and TDESs, consequently affects the refractive indices of DESs and TDESs. In the case of
233 DESs, the refractive index values of PC-GL DESs were higher than those of PC-EG DESs at all
234 temperatures. Indeed, components with higher density value had the higher refractive index value
235 whether single components or DESs. Furthermore, with an increase in mole fraction of HDSs in the
236 DESs, the refractive indices decreased. Also, as the molecular weight of DESs decreased, the amount

of refractive index of DESs decreased at all temperatures. These behaviors are similar to density and molar volume trends.

Similar to density, by adding AMPD to the binary mixture of PC-EG 1:10, the refractive index of $TDES_1$ (PC-EG-AMPD 1:10:1) witnessed a decreasing trend in the value. For example, refractive index of PC-EG 1:10 was 1.436820 at 343.15 K, while that of PC-EG-AMPD 1:10:1 was 1.441313 at the same temperature. This trend almost can be seen in the case of PC-GL-AMPD 1:16:1 ($TDES_2$) which had the higher values of refractive index than PC-GL 1:16 at all temperatures except for 293.15 and 298.15 K.

The experimental refractive index was fitted linearly by Equation (7),

$$n_D = a + b.(T) \quad (7)$$

where n_D is the refractive index, T is the temperature in Kelvin, and a and b are constants parameters that depend upon the salt/HBD molar ratio in the DESs and TDESs. In order to derive constant parameters (a and b) of Equation (7), the method of least-squares was applied using the Levenberg-Marquardt algorithm. Table 6 displays the values of a and b for the DESs and TDESs along with *RMSE* and R^2 values. The correlated refractive index data by Equation (7) were compared with experimental refractive index data. The results of this comparison are shown in Figure 6 for all DESs and TDESs studied in this work. From Figure 6, it can be evident that the predicted refractive index data by Equation (7) was in a well agreement with the experimental refractive index data with R^2 values of >0.999.

Table 5 . Experimental refractive index, n_D, of pure EG, pure GL, DESs and TDESs at several temperatures. Measurements were conducted within temperature range from T = (293.15 to 343.15) K and p = 0.1 MPa.

	DESs and TDESs						**Pure component**	
	DES_1	**DES_2**	**$TDES_1$**	**DES_3**	**DES_4**	**$TDES_2$**	**EG**	**GL**
T/K	Refractive index (n_D)							
293.15	1.447911	1.442980	1.452929	1.485031	1.478006	1.478364	1.431854	1.47333
298.15	1.446742	1.441660	1.451678	1.484014	1.476910	1.477329	1.430964	1.47182
303.15	1.445517	1.440463	1.450430	1.483051	1.475779	1.476244	1.429986	1.47035
308.15	1.444306	1.438892	1.449145	1.482050	1.474620	1.475165	1.429202	1.46887
313.15	1.443077	1.437701	1.447884	1.481045	1.473534	1.474074	1.428224	1.46747
318.15	1.441843	1.436381	1.446616	1.480204	1.472390	1.473101	1.427371	1.46597
323.15	1.440510	1.435027	1.445319	1.479201	1.471324	1.472129	1.426395	1.46456
328.15	1.439302	1.433762	1.444002	1.478246	1.470150	1.471006	1.425552	1.46312
333.15	1.438028	1.432379	1.442630	1.477131	1.469028	1.469859	1.424631	1.46161
338.15	1.436820	1.431223	1.441313	1.476176	1.4678600	1.468736	1.423742	1.46029
343.15	1.435546	1.429938	1.439941	1.475061	1.4667020	1.467589	1.422812	1.45867

Preprints (www.preprints.org) | NOT PEER-REVIEWED | Posted: 19 May 2017 doi:10.20944/preprints201705.0148.v1

258

259

Table 6 . The constant parameters of *a*, *b* used in Equation (3), *RMSE* and R^2 values.

DES	*a*	$10^3.b$	$10^5.RMSE$ [a]	R^2 [b]
DES$_1$	1.521	-0.2483	4.373	0.9999
DES$_2$	1.52	-0.262	8.170	0.9996
TDES$_1$	1.529	-0.2593	6.942	0.9997
DES$_3$	1.543	-0.1971	7.204	0.9995
DES$_4$	1.544	-0.2257	3.123	0.9999
TDES$_2$	1.541	-0.2139	7.590	0.9996

260

261

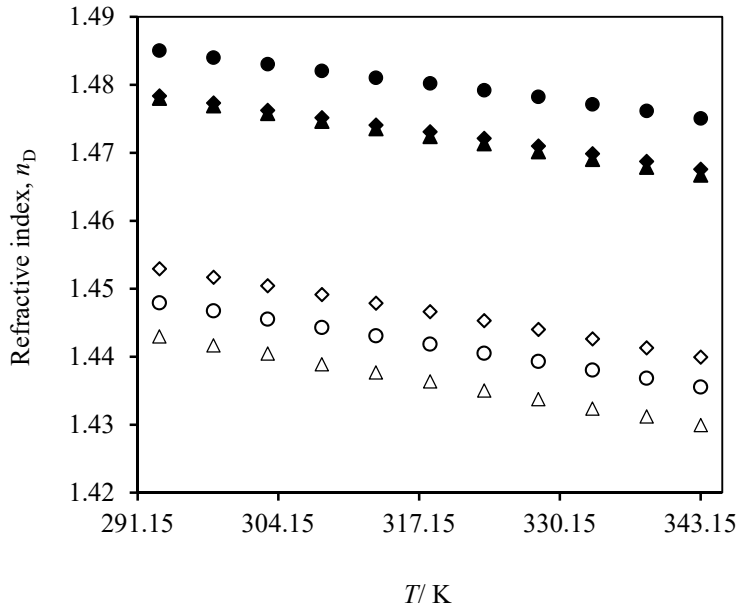

Figure 5. Refractive index, n_D, of the pure GL, pure EG, DESs and TDESs as a function of temperature. The symbols are the same as symbols depicted in Figure 1.

262

263

264

265

Preprints (www.preprints.org) | NOT PEER-REVIEWED | Posted: 19 May 2017 doi:10.20944/preprints201705.0148.v1

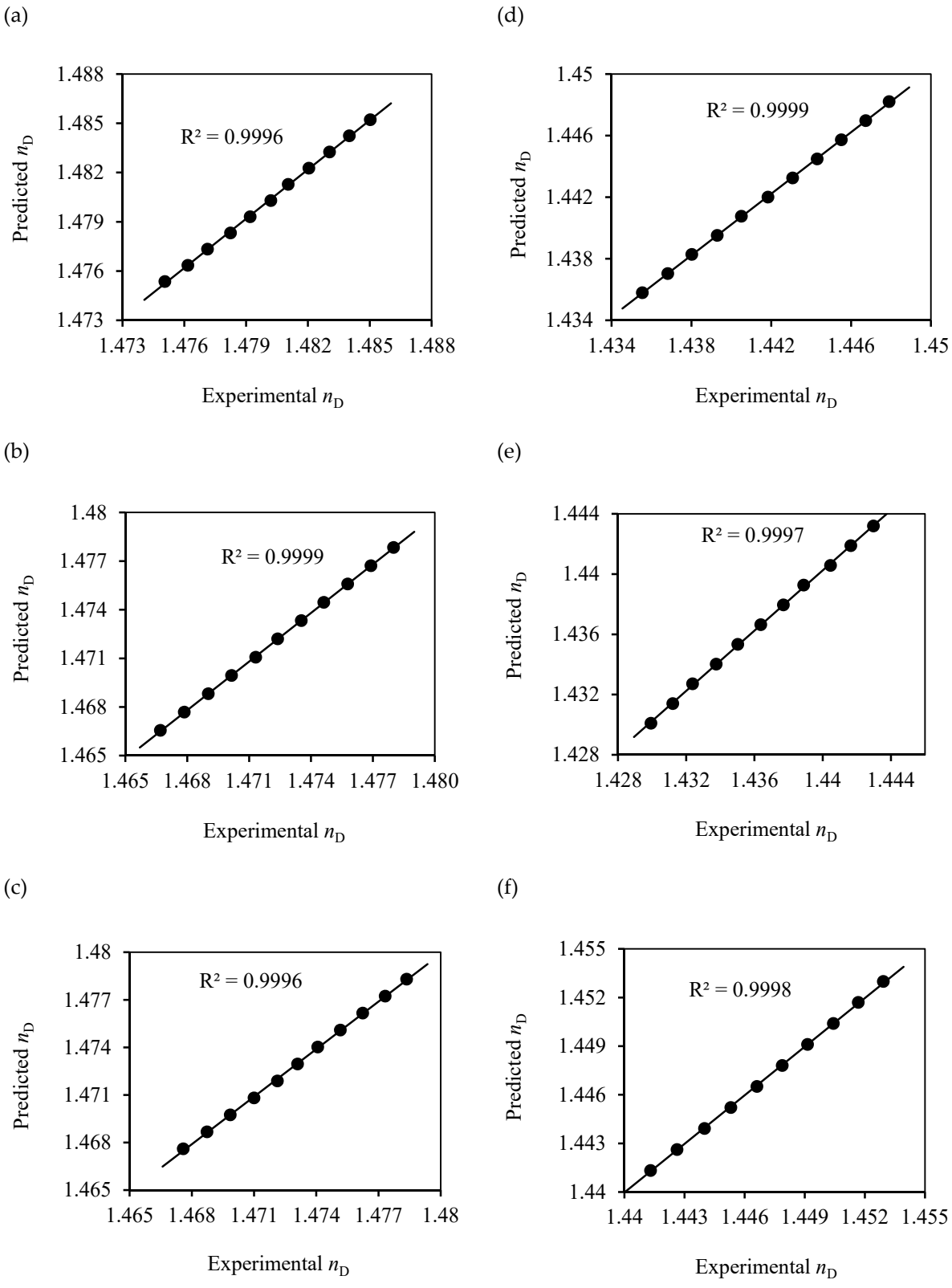

Figure 6. Comparison between the experimental and calculated values of referacrive index, n_D, for all DESs and TDESs: (a), DES_1; (b), DES_2; (c), $TDES_1$, (d), DES_3; (e), DES_4; (f), $TDES_2$.

 doi:10.20944/preprints201705.0148.v1

The molar refraction, R_m /($cm^3.mol^{-1}$), is a measure of the polarizability of a substance. The knowledge of specific refraction, R_D /($g^{-1}.cm^3$), molar refraction and electronic polarization, E, and polarizability constant, δ, of solvents play a vital role in many fields such as chemical, medical, biotechnical and engineering. Indeed, all of these properties are associated with refractive index. In the present work, all of the aforementioned properties of DESs and TDESs at several temperatures were calculated as following equations [30]:

$$E = n_D^2 \quad (8)$$

$$R_D = \frac{n_D^2 - 1}{n_D^2 + 2}.\frac{1}{\rho} \quad (9)$$

$$R_m = \frac{n_D^2 - 1}{n_D^2 + 2}.V \quad (10)$$

$$R_m = \frac{4}{3}\pi.N_A.\delta \quad (11)$$

where ρ, V and n_D are density, molar volume and refractive index of DESs and TDESs, respectively. δ is polarizability constant of liquid DESs and TDESs. N_A is Avogadro constant.

In order to study the forces between molecules and their behavior in solutions, extraction of E data is important [31]. Since E is power state of refractive index, it is expected that with an increase in temperature, the amount of electronic polarization of DESs and TDESs decreased. Similarly, this matter was observed when the molar ratio of DESs increased, as shown in Figure 7. The E values for PC-GL 1:10 and PC-EG 1:10 were 2.2023 and 2.0931 at 298.15 K, respectively. After the increasing mole fraction HBDs in DESs, these values for PC-GL 1:16 and PC-EG 1:16 decreased to 2.1813 and 2.0784 at the same temperature, respectively.

On the other hand, by adding AMPD to binary DESs, the values of E for both TDESs almost increased compared with those of binary DESs. For example, the E value for PC-GL 1:10 was 2.0931while that of PC-EG-AMPD 1:10:1 ($TDES_2$) was 2.1074 at 298.15 K.

Preprints (www.preprints.org) | NOT PEER-REVIEWED | Posted: 19 May 2017 doi:10.20944/preprints201705.0148.v1

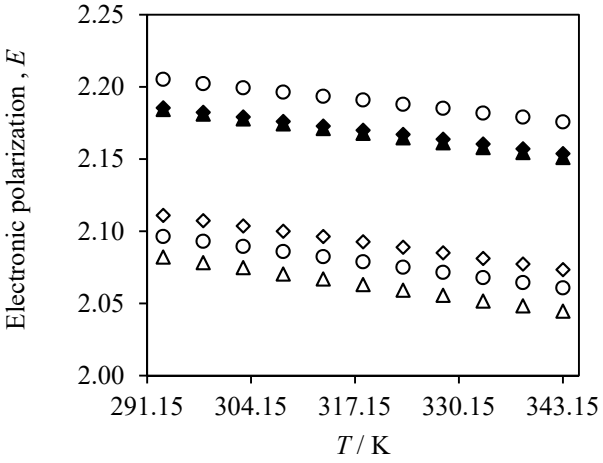

Figure 7. Electronic polarization, *E*, of DESs and TDESs with various molar ratios at several temperatures. The symbols are the same as symbols depicted in Figure 1.

Figure 8 displays the specific refraction, R_D, of DESs and TDESs. As can be seen, molar ratio salt/HBDs had a significant effect on the specific refraction of DESs. As the molar ratio increased this property decreased at all temperatures. However, temperature had not a great effect on R_D and an increase in temperature from 293.15 K to 343.15 K, brought about a minimal increase in the amount of R_D for all DESs and TDESs. As can be seen from Figure 8, there was a slight upward trend on the specific refraction of all DESs and TDESs by increasing temperature. In the case of TDESs, their R_D values decreased in comparison to their corresponding binary DESs, though this decreasing in R_D value for PC-GL-AMPD 1:16:1(TDES$_2$) occurred after 313.15 K.

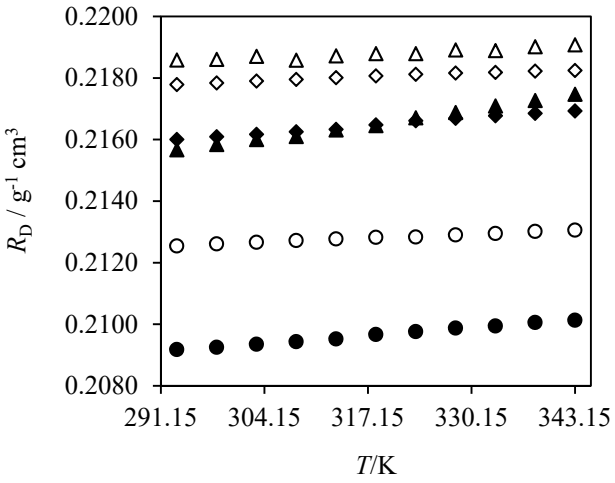

Figure 8. Specific refraction, R_D, of DESs and TDESs with various molar ratio at several temperatures. The symbols are the same as symbols depicted in Figure 1.

 doi:10.20944/preprints201705.0148.v1

Table 7 represents the numerical values of molar refraction, R_m, of DESs and TDESs and Figure 9 depicts these values against various temperatures. Although, temperature had not a great effect on R_m of DESs and TDESs, the effect of molar ratio was clear on R_m of DESs. In the case of PC-EG DESs, as the molar ratio increased from 1:10 to 1:16 salt to HBD, the R_m values decreased marginally. However, there was an increase in the R_m values of PC-GL DESs when the molar ratio increased.

From the data listed in Table 7 and shown in Figure 9, it is obvious that by adding AMPD as a third part to binary DESs, the R_m values of both TDESs increased compared with their corresponding binary DES. For example, PC-GL 1:16 (DES_4) had the R_m value of 20.4623 $cm^3.mol^{-1}$ at 298.15 K, in contrast the R_m value for PC-GL-AMPD 1:16:1 ($TDES_2$) was 20.6104 $cm^3.mol^{-1}$ at the same temperature.

Table 7 . Calculated molar refraction, R_m, of DESs and TDESs within temperature range from T = (293.15 to 343.15) K and p = 0.1 MPa.

	DESs and TDESs					
	DES_1	**DES_2**	**$TDES_1$**	**DES_3**	**DES_4**	**$TDES_2$**
T / K	R_m /($cm^3.mol^{-1}$)					
293.15	14.6635	14.5464	15.6815	20.1401	20.4460	20.6018
298.15	14.6684	14.5477	15.6854	20.1473	20.4623	20.6104
303.15	14.6720	14.5544	15.6900	20.1567	20.4774	20.6176
308.15	14.6759	14.5460	15.6936	20.1649	20.4869	20.6255
313.15	14.6795	14.5556	15.6977	20.1732	20.5069	20.6332
318.15	14.6830	14.5603	15.7019	20.1873	20.5202	20.6468
323.15	14.6838	14.5602	15.7055	20.1962	20.5444	20.6597
328.15	14.6885	14.5682	15.7085	20.2072	20.5608	20.6676
333.15	14.6915	14.5667	15.7101	20.2139	20.5809	20.6750
338.15	14.6962	14.5752	15.7131	20.2249	20.5977	20.6829
343.15	14.6991	14.5794	15.7147	20.2317	20.6166	20.6904

Preprints (www.preprints.org) | NOT PEER-REVIEWED | Posted: 19 May 2017 doi:10.20944/preprints201705.0148.v1

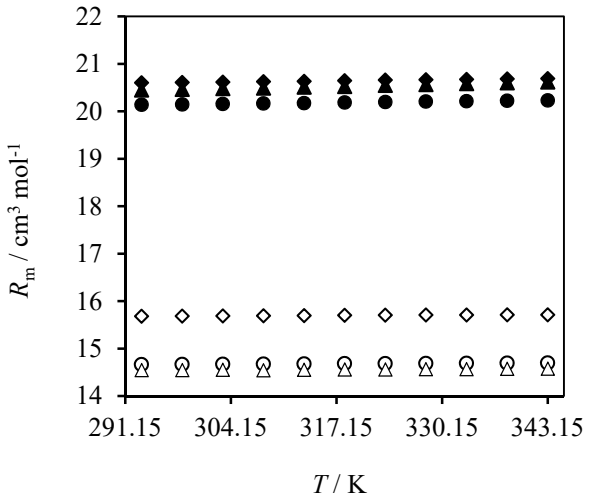

Figure 9. Molar refraction, R_m, of DESs and TDESs with various molar ratio at several temperatures. The symbols are the same as symbols depicted in Figure 1.

Tariq et al. [31] used Eq (15) for calculating the free volume, f_m, phosphonium-based ionic liquids. Sine, DESs and TDESs are defined as ionic liquid analogues, this equation was used to calculate the free volume of DESs.

$$f_m = V - R_m \quad (12)$$

where V is molar volume in cm^3.mol^{-1}; R_m is molar refraction in cm^3.mol^{-1}. Table 8 represents free volume of all DESs and TDESs at several temperatures. From Table 8, it is clear that with an increase in temperature all DESs and TDESs witnessed a gradual rise in the free volume. Further, by increasing molar ratio (from 1:10 to 1:16), the free volume all DESs increased. Amongst DESs with the same molar ratio, DESs with GL in their structure had the higher free volume. This may be explained by the fact that the higher alkyl chain on HBDs. From the Figure 11, it can be seen that GL has an additional CH in its structure and consequently caused the higher free volume. Moreover, by adding AMPD in binary DESs to form TDESs, the free volume of both TDESs increased compared with their corresponding binary DESs.

Preprints (www.preprints.org) | NOT PEER-REVIEWED | Posted: 19 May 2017 doi:10.20944/preprints201705.0148.v1

Table 8 . Calculated free volume, f_m, of DESs and TDESs within temperature range from T = (293.15 to 343.15) K and p = 0.1 MPa.

	DESs and TDESs					
	DES$_1$	**DES$_2$**	**TDES$_1$**	**DES$_3$**	**DES$_4$**	**TDES$_2$**
T / K	f_m/(cm^3.mol^{-1})					
293.15	40.1210	40.3248	42.3442	50.1280	51.7837	52.1319
298.15	40.2587	40.4709	42.4937	50.2719	51.9672	52.2885
303.15	40.3994	40.6193	42.6456	50.4153	52.1530	52.4488
308.15	40.5405	40.7675	42.7998	50.5610	52.3290	52.6109
313.15	40.6832	40.9254	42.9538	50.7079	52.5234	52.7751
318.15	40.8271	41.0848	43.1096	50.8496	52.7090	52.9393
323.15	40.9754	41.2352	43.2679	50.9989	52.9133	53.1023
328.15	41.1216	41.3998	43.4281	51.1483	53.1132	53.2734
333.15	41.2711	41.5515	43.5916	51.3080	53.3165	53.4475
338.15	41.4189	41.7070	43.7536	51.4588	53.5186	53.6204
343.15	41.5702	41.8658	43.9191	51.6200	53.7258	53.7963

Extraction of the refraction index and polarizability, δ, values of DESs and TDESs as a solvent media are important because having access to this data can give vital information about the behavior of DESs and TDESs such as dispersion forces. Indeed, a solvent with a large δ value has the strong dispersion forces [31]. The δ values of DESs and TDESs are shown in Table 9. From Table 9, it is clear that there was a decrease in the δ value of DESs as the molar ratio of DESs increased. Also, the δ values for both TDESs were lower than those of their corresponding binary DESs. For example, the δ values for PC-GL 1:16 (DES$_4$) and PC-GL-AMPD 1:16:1 (TDES$_2$) were 1.7078 10^{-23} and 1.611310^{-23} cm^3.mol^{-1} at 298.15 K. Furthermore, there was a marginal increase in the δ values of DESs and TDESs, as the temperature increased.

Table 9

Calculated polarizability constant, δ, of DESs and TDESs within temperature range from T = (293.15 to 343.15) K and p = 0.1 MPa.

	DESs and TDESs					
T / K	**DES$_1$**	**DES$_2$**	**TDES$_1$**	**DES$_3$**	**DES$_4$**	**TDES$_2$**
	10^{23} δ/(cm^3.mol^{-1})					
293.15	1.6848	1.3099	1.2064	2.0281	1.7074	1.6111
298.15	1.6856	1.3102	1.2066	2.0289	1.7078	1.6113
303.15	1.6865	1.3105	1.2070	2.0297	1.7081	1.6115
308.15	1.6874	1.3108	1.2072	2.0306	1.7085	1.6120
313.15	1.6883	1.3111	1.2076	2.0314	1.7088	1.6124

318.15	1.6892	1.3113	1.2078	2.0322	1.7092	1.6127
323.15	1.6901	1.3117	1.2080	2.0329	1.7095	1.6132
328.15	1.6909	1.3120	1.2081	2.0337	1.7099	1.6136
333.15	1.6918	1.3123	1.2084	2.0343	1.7102	1.6140
338.15	1.6927	1.3126	1.2088	2.0351	1.7105	1.6144
343.15	1.6936	1.3129	1.2090	2.0359	1.7109	1.6148

2.4. Internal pressure of DESs

One of the major properties of liquids is internal pressure, P_{int}. Extraction of internal pressure values is of the utmost importance because this property affected many properties of liquids including ultrasonic velocity, free volume, viscosity, surface tension, solubility parameter and so on [31; 32]. Generally, internal pressure of a liquid is defined as,

$$P_{int} = \left(\frac{\delta U}{\delta V}\right)_T \quad (13)$$

where P_{int} is internal pressure in Pa which shows the change in internal energy of one mole of solvent with respect to molar volume of liquid at the constant temperature. Indeed, P_{int} reflects generally dispersion, repulsion, and dipole–dipole interactions in the solvent which vary most rapidly near the equilibrium molecular separation [33]. Using the molar refraction and molar volume data, the internal pressure of DESs and TDESs is calculated through the Buchler–Hirschfelder–Curtis equation of state at the given temperature, as defined [31; 34; 35],

$$P_{int} = \frac{2^{1/6} RT}{2^{1/6} V - d.N_A^{1/3} V^{2/3}} \quad (14)$$

where P_{int} is internal pressure in MPa; R and T are the gas constant in $J.K^{-1}.mol^{-1}$ and temperature in Kelvin, respectively; N_A is Avogadro constant in mol^{-1}; V is the molar volume of DESs and TDESs in $cm^3.mol^{-1}$; d is the molecular radius in cm, which can be defined as the following equation,

$$d = 2\left(\frac{3R_m}{4\pi N_A}\right)^{1/3} \quad (15)$$

where R_m is the molar refraction in $cm^3.mol^{-1}$; R and T are the gas constant and temperature in Kelvin; N_A is Avogadro constant in mol^{-1}.

The internal pressures of DESs and TDESs are shown in Table 10 and depicted in Figure 10 against different temperatures. These results reveal that DESs and TDESs can be considered as the class of liquids which have the positive temperature coefficients of internal pressure. That is, internal pressure of DESs and TDESs increased with raising temperature, in the defined temperature range. According to Figure 10, there was an increasing trend on the internal pressure values of DESs and TDESs when the temperature was increased. However, the effect of molar ratio on internal pressure was different. The amount of internal pressure of all DESs decreased as the molar ratio increased. For instance, PC-EG 1:10 had P_{int} value of 156.6580 MPa at 298.15 K, but by increasing the amount of EG in DES, this value for PC-EG 1:16 was 155.1311 MPa at the same temperature.

Preprints (www.preprints.org) | NOT PEER-REVIEWED | Posted: 19 May 2017 doi:10.20944/preprints201705.0148.v1

It worthy to investigate the effect of alkyl chain lengths on the internal pressure of DESs. It can be clearly evident from Figure 10 that DESs with EG in their structure at the same molar ratios had the higher P_{int} values rather than DESs with GL in their structures at all temperatures studied here. Indeed, GL has an additional CH in its structure, as shown in Figure 11; then DESs having GL in structure had the lower P_{int} values. This matter has been well established in the case of ILs [33]. Further, the P_{int} values of TDESs were even lower than those of binary DESs. The decreasing was more obvious in the case of PC-EG-AMPD 1:10:1 ($TDES_1$) rather than PC-GL-AMPD 1:16:1 ($TDES_2$).

Table 10 . Calculated internal presure, P_{int}, of DESs and TDESs within temperature range from T = (293.15 to 343.15) K and p = 0.1 MPa.

	DESs and TDESs					
	DES_1	**DES_2**	**$TDES_1$**	**DES_3**	**DES_4**	**$TDES_2$**
T / K	P_{int}/MPa					
293.15	154.7205	153.2630	147.2526	127.9432	123.0968	122.3129
298.15	156.6580	155.1311	149.0718	129.6383	124.6351	123.9146
303.15	158.5571	156.9879	150.8645	131.3274	126.1491	125.4885
308.15	160.4379	158.7733	152.6257	132.9928	127.6690	127.0453
313.15	162.2910	160.5557	154.3726	134.6413	129.1374	128.5823
318.15	164.1197	162.2937	156.0941	136.3100	130.6064	130.1193
323.15	165.8977	164.0434	157.7847	137.9262	132.0237	131.6465
328.15	167.6843	165.7304	159.4475	139.5349	133.4245	133.1230
333.15	169.4287	167.4329	161.0722	141.0827	134.8081	134.5756
338.15	171.1720	169.1354	162.6923	142.6613	136.1749	136.0209
343.15	172.8730	170.7874	164.2741	144.1780	137.5154	137.4422

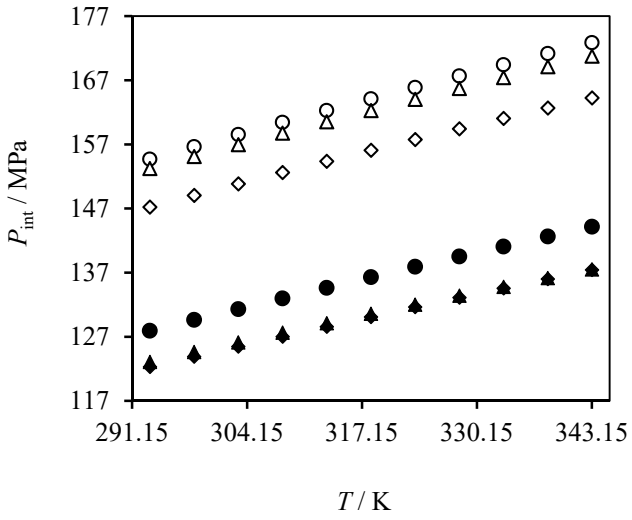

Figure 10. Internal pressure, P_{int}, of DESs and TDESs with various molar ratios at several temperatures. The symbols are the as symbols depicted in Figure 1.

Preprints (www.preprints.org) | NOT PEER-REVIEWED | Posted: 19 May 2017 doi:10.20944/preprints201705.0148.v1

3. Materials and Methods

3.1 Chemicals

Potassium carbonate (PC) with >99.9% purity and 2-amino-2methyl-1-3-propanediol (AMPD) with >99% purity were supplied by Sigma-Aldrich; glycerol (GL) with >99.8 %purity and ethylene glycol (EG) >99.5% purity were purchased from *R&M* Chemicals supplier. Table 11 represents the abbreviation of these chemicals and DESs along with molar ratios, symbol and molecular weight of each component and DESs. In order to prevent moisture and any contamination, all materials were kept in a controlled environment. Figure 11 shows the molecular structure of the PC and the HBDs. In this study, DES_1 and DES_2 represent PC-EG 1:10 and PC-EG 1:16, respectively; DES_3, DES_4 show PC-GL 1:10 and PC-GL 1:16, respectively; $TDES_1$ and $TDES_2$ represent PC-EG-AMPD 1:10:1 and PC-GL-AMPD 1:16:1, respectively.

Table 11 . The abbreviations, molecular weights and molar ratios for components and DESs and TDESs in this work.

DES/TDES		Salt		HBD		Molar ratio	
Symb. [a]	$M_{DES/TDES}$ [b]	Abb. [c]	M_{salt} [d]	Abb. [c]	M_{HBD} [e]	Salt	HBD
PC-EG (DES_1)	68.992	PC	138.21	EG	62.07	1	10
PC-EG (DES_2)	66.549	PC	138.21	EG	62.07	1	16
PC-EG- AMPD ($TDES_1$)	72.004	PC	138.21	EG & AMPD	62.07 105.14	1	10:1
PC-GL(DES_3)	96.283	PC	138.21	GL	92.09	1	10
PC-GL(DES_4)	94.803	PC	138.21	GL	92.09	1	16
PC-GL- AMPD ($TDES_2$)	95.377	PC	138.21	GL & AMPD	92.09 105.14	1	16:1

[a] Symbol.

[b] M_{DES} molecular weight of DES and TDES in g·mol^{-1} was calculated according to AlOmar et al. [8].

[c] Abbreviation.

[d] Molecular weight of salt in g·mol^{-1}.

[e] Molecular weight of HBD in g·mol^{-1}.

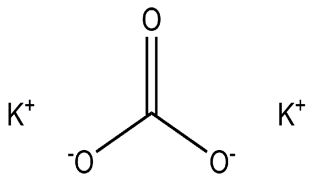

Potassium Carbonate (PC)

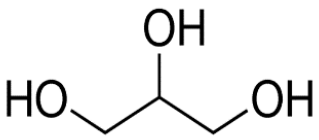

Glycerol (GL)

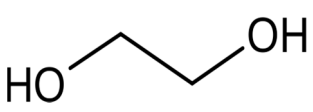

Ethylene glycol (EG)

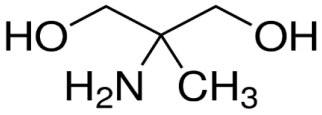

2-amino-2methyl-1-3-propanediol (AMPD)

Figure. 11. A schematic of chemical structure of the salt and HBDs.

 doi:10.20944/preprints201705.0148.v1

3.2 DES preparation

Binary DESs were prepared with the ratios of 1:10 for PC to EG and 1:16 for PC to GL. In order to form ternary TDESs, a type of hindered amine (HA) called 2-amino-2methyl-1-3-propanediol (AMPD) was mixed with the binary mixtures with the molar ratios of 1:10:1 for PC-EG-AMPD and 1:16:1 for PC-GL-AMPD. The weight measurements of pure components of all DESs and TDESs were performed in a digital balance (Sartorius, model BSA 224S-CW) with an uncertainty of ±0.1 mg. The salts were mixed with related HBDs using magnetic stirrer at 350 rpm, atmospheric pressure and the temperature of 333.15 to 353 K for 1-2 h in a fume hood until a homogeneous and uniform liquid without any precipitate was formed. For preparation of TDESs, after 15-30 minutes mixing the binary mixtures, AMPD as a ternary part was immediately added to binary mixture while stirring. The heating of ternary mixture continued more than 1h. The formed DESs and TDESs were kept in the tight bottles to prevent any contamination with atmospheric water vapor. The DESs and TDESs were used without any further purification. Since DESs and TDESs are known as the hygroscopic solvents, their water contents were measured using a Mettler Toledo Karl-Fischer (C30) after preparation. It was found that the water content of DESs and TDESs is less than 0.2 wt%. The DESs and TDESs were used without any further purification.

3.3 Density measurement

A digital density meter (Anton Par, model, DMA-4500M) was applied to measure the density of HBDs, DESs and TDESs with an accuracy of $\pm 5\times10^{-5}$ g.cm^{-3}, and a temperature control accuracy of ±0.01 K. The density meter works on the principle of oscillating U-tube method. In order to gain accurate results and remove any unwanted particles, the U-shaped tube of density meter was cleaned by acetone and standard water of millipore quality. An air blower was used to dry the moisture content inside the tube and avoid any influence on the results. Density of all DESs and TDESs was measured in three runs at atmospheric pressure and temperatures raising from 293.15 to 343.15 K and the average value was reported for the further study.

3.4 Refractive index measurement

Refractive index of HBDs, DESs and TDESs were measured by means of a digital Abbemat automatic refractometer (Anton Par, model WR), with an accuracy of $\pm 4\times10^{-5}$ n_D, and a temperature control accuracy of ±0.03 K. In order to obtain accurate and reliable data, standard water of millipore quality was utilized to calibrate the refractometer. Before pouring the sample into the sample mold, the prism face was carefully cleaned with ethanol and dried to prevent any disturbance in the results because of possible minute sediments on the prism face. Experimental refractive index of DESs and TDESs was measured three times at atmospheric pressure and temperature ranging from 293.15 to 343.15 K with a regular interval of 5 K at wavelength of 589.3 nm. All refractive index values were reported in the average experimental values.

4. Conclusions

In this work, the binary DESs were PC-GL with molar ratios 1:10 and 1:16 and PC-EG with the same molar ratios. TDESs were prepared by adding AMPD in binary DESs such as PC-GL-AMPD

1:16:1 and PC-EG-AMPD 1:10:1. The experimental density and refractive index of all DESs, TDESs and their HBDs were measured at the temperature of 293.15 to 343.15 K with an interval of 5 K. The effect of temperature, molar ratio, type of HBD and molecular weight was investigated on the properties. The results revealed that as the temperature increases, the density and refractive index values of DESs and TDESs decrease. Moreover, the molar ratio had an effect on these properties DESs. By increasing amount of HBDs in DESs the density and refractive index values of DESs decreased toward the properties of their HBD. By adding AMPD to the binary DES of PC-GL 1:16 the density and refractive index of PC-GL-AMPD 1:16:1 ($TDES_2$) increased at all temperatures except for density at 293.15 and 298.15 K. The density of PC-EG-AMPD 1:10:1 ($TDES_1$) decreased at all temperatures by adding AMPD to the binary DES of PC-EG 1:10, while the refractive index of this $TDES_1$ increased at the same temperatures. It was found that DESs with the GL in their structures had the higher density and refractive index values in comparison to DESs having EG in their structures with same molar ratios. Finally, there was a decrease in the density and refractive index of DESs (with the same components but different molar ratios) when the molecular weight decreased.

References

1. Abbott A. P.; Capper G.; Davies D. L.; Rasheed R. K., and Tambyrajah V. Novel solvent properties of choline chloride/urea mixtures. *Chem. Commun.* **2003**, 70-71.
2. Hayyan A.; Mjalli F. S.; Alnashef I. M.; Al-Wahaibi T.; Al-Wahaibi Y. M., and Hashim M. A. Fruit sugar-based deep eutectic solvents and their physical properties. *Thermochim. Acta* **2012**, 541, 70-75.
3. Kareem M. A.; Mjalli F. S.; Hashim M. A., and Alnashef I. M. Phosphonium-based ionic liquids Analogues and their physical properties. *J. Chem. Eng. Dat* **2010**, 55, 4632-4637.
4. Leron R. B.; Soriano A. N., and Li M.-H. Densities and refractive indices of the deep eutectic solvents (choline chloride + ethylene glycol or glycerol) and their aqueous mixtures at the temperature ranging from 298.15 to 333.15 K. *J. Taiwan Inst. Chem. Eng.* **2012**, 43, 551-557.
5. Leron R. B. and Li M.-H. High-pressure density measurements for choline chloride: Urea deep eutectic solvent and its aqueous mixtures at T = (298.15 to 323.15) K and up to 50 MPa. *J. Chem. Thermodyn.* **2012**, 54, 293-301.
6. Mjalli F. S.; Naser J.; Jibril B.; Al-Hatmi S. S., and Gano Z. S. Ionic liquids analogues based on potassium carbonate. *Thermochim. Acta* **2014**, 575, 135-143.
7. Siongco K. R.; Leron R. B., and Li M.-H. Densities, refractive indices, and viscosities of N,N-diethylethanol ammonium chloride–glycerol or –ethylene glycol deep eutectic solvents and their aqueous solutions. *J. Chem. Thermodyn.* **2013**, 65, 65-72.
8. Alomar M. K.; Hayyan M.; Alsaadi M. A.; Akib S.; Hayyan A., and Hashim M. A. Glycerol-based deep eutectic solvents: Physical properties. *J. Mol. Liq.* **2016**, 215, 98-103.
9. Yadav A. and Pandey S. Densities and viscosities of (Choline Chloride + Urea) deep eutectic solvent and its aqueous mixtures in the temperature range 293.15 K to 363.15 K. *J. Chem. Eng* **2014**, 59, 2221-2229.
10. Liu B. and Liu Y. Physical Properties of Aqueous mixtures of acetamide-LiCl eutectic ionic liquids as a function of temperature and composition. *Asian J. Chem.* **2014**, 26, 8557-8562.

11. Florindo C.; Oliveira F. S.; Rebelo L. P. N.; Fernandes A. M., and Marrucho I. M. Insights into the synthesis and properties of deep eutectic solvents based on cholinium chloride and carboxylic acids. *ACS Sustainable Chem. Eng.* **2014**, 2, 2416-2425.
12. Nkuku C. A. and Lesuer R. J. Electrochemistry in deep eutectic solvents. *J. Phys. Chem.* **2007**, 111, 13271-13277.
13. Maugeri Z. and Dominguez De Maria P. Novel choline-chloride-based deep-eutectic-solvents with renewable hydrogen bond donors: levulinic acid and sugar-based polyols. *RSC Adv.* **2012**, 2, 421-425.
14. Dai Y.; Van Spronsen J.; Witkamp G.-J.; Verpoorte R., and Choi Y. H. Natural deep eutectic solvents as new potential media for green technology. *Anal. Chim. Acta* **2013**, 766, 61-68.
15. Wang H.; Jia Y.; Wang X.; Yao Y., and Jing Y. Physical–chemical properties of nickel analogs ionic liquid based on choline chloride. *J. Therm. Anal. Calorim* .**2014**, 115, 1779-1785.
16. Liu Y.-T.; Chen Y.-A., and Xing Y.-J. Synthesis and characterization of novel ternary deep eutectic solvents. *Chin. Chem. Lett.* **2014**, 25, 104-106.
17. Sze L. L.; Pandey S.; Ravula S.; Pandey S.; Zhao H.; Baker G. A., and Baker S. N. Ternary deep eutectic solvents tasked for carbon dioxide capture. *ACS Sustainable Chem. Eng.* **2014**, 2, 2117-2123.
18. Khezeli T. and Daneshfar A. Synthesis and application of magnetic deep eutectic solvents: Novel solvents for ultrasound assisted liquid-liquid microextraction of thiophene. *Ultrason. Sonochem* (in press).
19. Sarkar S. and Sampath S. Ambient temperature deposition of gallium nitride/gallium oxynitride from a deep eutectic electrolyte, under potential control. *Chem. Commun.* **2016**, 52, 6407-6410.
20. García G.; Aparicio S.; Ullah R., and Atilhan M. Deep eutectic solvents: physicochemical properties and gas separation applications. *J. Am. Chem. Soc.* **2015**, 29, 2616-2644.
21. Nayak J. N.; Aralaguppi M. I., and Aminabhavi T. M. Density, viscosity, refractive index, and speed of sound in the binary mixtures of 1,4-Dioxane + Ethanediol, + Hexane, + Tributylamine, or + Triethylamine at (298.15, 303.15, and 308.15) K. *Chem. Eng. Data* **2003**, 48, 1152-1156.
22. Cristancho D. M.; Delgado D. R.; Martínez F.; Abolghassemi Fakhree M. A., and Jouyban A. Volumetric properties of glycerol + water mixtures at several temperatures and correlation with the Jouyban-Acree model. *Revista Colombiana de Ciencias Químico - Farmacéuticas* **2011**, 40, 92-115.
23. Aminabhavi T. M. and Banerjee K. Density, viscosity, refractive index, and speed of sound in binary mixtures of Methyl Acetate + Ethylene Glycol or + Poly(ethylene glycol) in the temperature interval (298.15−308.15) K. *Chem. Eng. Data* **1998**, 43, 852-855.
24. Tsierkezos N. G. and Molinou I. E. Densities and viscosities of ethylene glycol binary mixtures at 293.15 K. *Chem. Eng. Data* **1999**, 44, 955-958.
25. Vural U. S.; Muradoglu V., and Vural S. Excess molar volumes, and refractive index of binary mixtures of glycerol+ methanol and glycerol+ water at 298.15 K and 303.15 K. *Chem. Soc. Ethiop.* **2011**, 25, 111-118.
26. Koohyar F.; Rostami A. A.; Chaichi M. J., and Kiani F. Study on Thermodynamic properties for binary Systems of Water. *J. Chem.* **2012**, 2013,
27. Chemat F.; Anjum H.; Shariff A. M.; Kumar P., and Murugesan T. Thermal and physical properties of (Choline chloride + urea + l-arginine) deep eutectic solvents. *J. Mol. Liq.* **2016**, 218, 301-308.

 doi:10.20944/preprints201705.0148.v1

28. Abbott A. P.; Harris R. C.; Ryder K. S.; D'agostino C.; Gladden L. F., and Mantle M. D. Glycerol eutectics as sustainable solvent systems. *Green Chem*. **2011**, 13, 82-90.
29. Yaws C. L. Chemical Properties Handbook. first ed., McGraw-Hill Company, New York, USA, 1999. pp. 616-642.
30. Arun B. Nikumbh and Rathi M. V. Study of molar refraction and polarisability constant of aqueous solutions of NH_4NO_3 and $KBrO_3$ at different temperatures. *AJER* **2016**, 5, 195-200.
31. Tariq M.; Forte P. a. S.; Gomes M. F. C.; Lopes J. N. C., and Rebelo L. P. N. Densities and refractive indices of imidazolium- and phosphonium-based ionic liquids: Effect of temperature, alkyl chain length, and anion. *J. Chem. Thermodyn.* **2009**, 41, 790-798.
32. Goharshadi E. K. and Nazari F. Computation of internal pressure of liquids using a statistical mechanical equation of state. *Fluid Phase Equilib.* **2001**, 187–188, 425-431.
33. Singh T. and Kumar A. Temperature dependence of physical properties of imidazolium based ionic liquids: internal pressure and molar refraction. *J. Solution Chem.* **2009**, 38, 1043-1053.
34. Casás L. M.; Marino G.; Mascato E.; Iglesias M.; Orge B., and Tojo J. Excess molar internal pressures and changes in refractive indices of acetone + methanol + (2-methyl-1-propanol or 3-methyl-1-butanol) at 298.15 K. Phys. *Chem. Liq.* **2005**, 43, 473-483.
35. Zorębski E. Internal pressure in liquids and binary liquid mixtures. , *J. Mol. Liq.* **2009**, 149, 52-54.